

Published in final edited form as:

Neuropsychologia. 2012 July ; 50(8): 1759–1765. doi:10.1016/j.neuropsychologia.2012.03.033.

Age-related changes in parahippocampal white matter integrity: A diffusion tensor imaging study

E. Rogalski^a, G.T. Stebbins^b, C.A. Barnes^{c,d,e,f}, C.M. Murphyⁱ, T.R. Stoub^b, S. George^b, C. Ferrari^b, R.C. Shah^{g,h}, and L. deToledo-Morrell^{b,*}

^aCognitive Neurology and Alzheimer's Disease Center at Northwestern University, Feinberg School of Medicine, Chicago, IL, USA

^bDepartment of Neurological Sciences, Rush University Medical Center, Chicago, IL 60612, USA

^cDepartment of Psychology, University of Arizona, Tucson, AZ, USA

^dDepartment of Neurology, University of Arizona, Tucson, AZ, USA

^eArizona Research Laboratories, Division of Neural Systems, Memory and Aging, University of Arizona, Tucson, AZ, USA

^fEvelyn F. McKnight Brain Institute, University of Arizona, Tucson, AZ, USA

^gDepartment of Family Medicine, Rush University Medical Center, Chicago, IL, USA

^hRush Alzheimer's Disease Center, Rush University Medical Center, Chicago, IL, USA

ⁱDepartment of Medicine, University of Arizona, Tucson, AZ, USA

Abstract

The axons in the parahippocampal white matter (PWM) region that includes the perforant pathway relay multimodal sensory information, important for memory function, from the entorhinal cortex to the hippocampus. Previous work suggests that the integrity of the PWM shows changes in individuals with amnesic mild cognitive impairment and is further compromised as Alzheimer's disease progresses. The present study was undertaken to determine the effects of healthy aging on macro- and micro-structural alterations in the PWM. The study characterized *in vivo* white matter changes in the parahippocampal region that includes the perforant pathway in cognitively healthy young (YNG, $n = 21$) compared to cognitively healthy older (OLD, $n = 21$) individuals using volumetry, diffusion tensor imaging (DTI) and tractography. Results demonstrated a significant reduction in PWM volume in old participants, with further indications of reduced integrity of remaining white matter fibers. In logistic regressions, PWM volume, memory performance and DTI indices of PWM integrity were significant indicator variables for differentiating the young and old participants. Taken together, these findings suggest that age-related alterations do occur in the PWM region and may contribute to the *normal* decline in memory function seen in healthy aging by degrading information flow to the hippocampus.

Keywords

Magnetic resonance imaging; Aging; Memory; Tractography; Medial temporal lobe; Perforant pathway

1. Introduction

The hippocampus, entorhinal cortex (EC), and the parahippocampal region in general have been identified as critical neuroanatomical components of the medial temporal lobe memory system (Squire & Zola-Morgan, 1991; Young, Otto, Fox, & Eichenbaum, 1997). Neurons of the entorhinal cortex receive multimodal sensory information from primary sensory and association cortices (Amaral, Insausti, & Cowan, 1987; Van Hoesen & Pandya, 1975b; Van Hoesen, Pandya, & Butters, 1975) and relay this information to the hippocampus via the perforant pathway (Hyman, Van Hoesen, Damasio, & Barnes, 1984; Van Hoesen & Pandya, 1975a). The integrity of this white matter tract is crucial for proper information flow to the hippocampus and, thus, for memory function.

Recent *in vivo* magnetic resonance imaging (MRI) work from our laboratory demonstrated decreased parahippocampal white matter (PWM) volume, as well as tissue degradation as measured by diffusion tensor imaging (DTI), in the region of the perforant pathway in people with amnesic mild cognitive impairment (aMCI) who are at risk for developing Alzheimer's disease (AD; Rogalski et al., 2009; Stoub et al., 2006) and in those with mild AD (Wang et al., 2010). Similar results have been reported by other laboratories (Kalus et al., 2006; Salat et al., 2010). In addition, these PWM changes were found to be a significant predictor of memory function, suggesting that white matter integrity in the region of the perforant pathway is important for successful memory in humans.

Investigations in animal models of aging have demonstrated that the perforant pathway is altered as a function of the aging process. Although cell numbers remain the same in layer II of the entorhinal cortex, as well as in hippocampal CA3 and dentate gyrus regions (Rasmussen, Schliemann, Sorensen, Zimmer, & West, 1996), there is a reduction in actual synapse numbers in the middle molecular layer of the hippocampal dentate gyrus, especially in rodents with memory dysfunction (Geinisman, deToledo-Morrell, & Morrell, 1986; Geinisman, deToledo-Morrell, Morrell, Persina, & Rossi, 1992). Similarly, using synaptophysin immunofluorescence staining as a measure of synaptic loss, Smith, Adams, Gallagher, Morrison and Rapp (2000) also demonstrated alterations in hippocampal connectivity in memory impaired old rodents compared to those without memory dysfunction. In addition, electrophysiological experiments have shown a decrease in the pre-synaptic fiber potential in old rats with age-related memory impairments (Barnes, 1979; Barnes & McNaughton, 1980), suggesting a pruning of axon collaterals from the perforant pathway to the dentate gyrus. If there is a cross-species correspondence in the types of brain changes that occur during aging, then the rodent data predict that humans should also show alterations in the region of the perforant pathway as a function of normal aging. Such changes would be further accentuated by pathological processes predictive of AD.

In fact, a recent investigation from our laboratory has demonstrated that white matter volume changes in the perforant pathway region of the PWM do take place as a function of the aging process in humans (Stoub et al., 2011). It is possible that in addition to age-related volumetric changes, there are micro-structural alterations in remaining fibers in this region that would affect information flow from the entorhinal cortex to the hippocampus. Such micro-structural alterations can be detected *in vivo* using diffusion tensor imaging (DTI). This technique combines MR diffusion-weighted pulse sequences with tensor mathematics to measure molecular diffusion in three dimensions. Commonly used DTI metrics include mean diffusivity (MD) and fractional anisotropy (FA). MD provides a measure of non-directional diffusion that can be used as a non-invasive proxy measure of the general integrity of tissue. An increase in MD reflects a decrease in the barriers of free diffusion that is thought to be a sign of tissue degradation. In contrast, FA is a scalar metric that describes the directionality of diffusion and offers information about the parallel organization of white

matter fibers (Moseley, 2002). In healthy white matter, FA is high because the direction of diffusion is parallel to axon fibers; decreases in FA occur when parallel diffusion is disrupted possibly due to demyelination or axonal damage.

Previous studies that examined age and disease related changes in white matter have reported alterations in FA and MD in multiple white matter regions not only in healthy aging (e.g., Abe et al., 2008; Brickman et al., 2011; Malykhin et al., 2011; Pfefferbaum et al., 2000; Salat et al., 2009; Sasson, Doniger, Pasternak, Tarrasch, & Assaf, 2011; Yassa, Muftuler, & Stark, 2010), but also in people with AD and in those at high risk for developing AD (Huang & Auchus, 2007; Huang, Friedland, & Auchus, 2007; Kalus et al., 2006; Kantarci et al., 2011; Medina et al., 2006; Rogalski et al., 2009; Salat et al., 2010; Wang et al., 2010).

The goal of the present diffusion tensor imaging study was to determine if, in addition to age-related volume loss, there are micro-structural alterations in remaining fibers, specifically in the PWM that includes the perforant pathway, in cognitively healthy older individuals compared to young participants. Such microstructural alterations in remaining fibers in this region could further degrade information flow from the entorhinal cortex to the hippocampus and affect memory function. In addition to DTI metrics of white matter integrity, we used tractography based on models of coherent directional diffusion across voxels. These models allow the examination of fiber integrity between two regions of interest (ROI) or of fibers passing through a given ROI.

2. Methods

2.1. Participants

Participants included 21 young (mean age = 25.04 years, range 21–30; 12 male and 9 female) and 21 older, cognitively healthy individuals (mean age = 71.5, range 65–86; 8 male and 13 female). We chose these age ranges to clearly separate the younger from the older participants. This specific design allowed us to examine young versus old differences in PWM macro- and micro-structural integrity as opposed to examining the relationship between age as a continuous variable and PWM integrity. Young (YNG) participants were recruited from Rush University Medical Center students and employees, as well as their friends and family members. The healthy older participants (OLD) were recruited from the community for an ongoing longitudinal imaging study (deToledo-Morrell et al., 2004; Stoub, Rogalski, Leurgans, Bennett, & deToledo-Morrell, 2010) and were evaluated at the Rush Alzheimer's Disease Center (RADC, Chicago, IL) clinic.

Older participants did not have any cognitive impairment or complaints of memory problems at entry into the study. The clinical evaluation carried out by the RADC has been described previously (deToledo-Morrell et al., 2004; Stoub et al., 2005). Briefly, the evaluation included the Consortium to Establish a Registry for Alzheimer's Disease (CERAD; Morris et al., 1989) procedures and included a medical history, neurological examination, neuropsychological testing, informant interview and blood tests as needed (Stoub et al., 2006). Selection of healthy old participants required a normal neurological examination, normal cognition as determined by performance on neuropsychological tests, a Mini Mental State Examination (MMSE; Folstein, Folstein, & McHugh, 1975) score ≥ 27 (out of a maximum of 30 points) and age ≥ 65 . Young subjects were screened with a questionnaire, received the same memory testing as the old participants (see below), as well as the MMSE. Subjects in both groups were excluded from entering the study if there were contra-indications for MR imaging, or if neurologic, psychiatric or systemic conditions, as well as a history of temporal lobe epilepsy that could affect medial temporal lobe structures,

were found. Informed consent was obtained from all participants according to the guidelines of the Institutional Review Board of Rush University Medical Center.

2.2. MRI acquisition and analysis

Imaging was performed on a 1.5 T General Electric scanner (General Electric Medical Systems, Milwaukee, WI, USA) with LX Horizon high-speed gradient upgrades (Rev 11.4) at Rush University Medical Center. Foam padding and tape were used to secure participants' head to minimize movement. The scanning session was completed in one visit and consisted of a locator scan, a 3D T1-weighted spoiled gradient recalled (SPGR) scan (124 contiguous 1.6 mm thick slices acquired in the coronal plane, matrix = 256×192 , field of view = 22 cm, TR/TE = 34/7 ms, flip angle = 35°), and a single-shot echo planar high resolution diffusion weighted scan (TR/TE = 12100/97 ms, field of view = 25 cm, matrix = 128×128 , 38 gapless 3mm slices, in-plane resolution = 1.95 mm, 2NEX, 3 repetitions). Two diffusion weights (b -values) were used: $b = 0$ and $b = 800$ s/mm². Diffusion encoding gradients were applied along a total of 24 non-collinear directions repeated six times for each slice. SPGR scans were converted from individual slices to volumes using the DICOM toolbox in SPM5 (Wellcome Department of Cognitive Neurology, London, UK).

Post-acquisition processing of DTI images utilized an open source suite of software developed at Stanford University (<http://sirl.stanford.edu/software>) with modifications developed in our laboratory. The initial processing of the DTI scans required un-warping of the eddy current distortions. Simple co-registration of the DTI images is not optimal for correcting these distortions; therefore, we utilized a correction method developed by Rohde, Barnett, Basser, Marengo, and Pierpaoli (2004). This algorithm combines a rigid-body 3D motion correction (6 parameters) with a constrained non-linear warping (8 parameters) based on a model of the expected eddy current distortions. Calculation of the DTI metrics proceeded from the un-warped DTI images through the calculation of the six diffusion coefficients defining the six elements of the diffusion tensor (Basser, Mattiello, & LeBihan, 1994). Eigenvectors, defining the three principle directions of diffusion and associated eigenvalues (λ_1 , λ_2 , λ_3) were calculated at each voxel yielding measures of MD and FA, as described by Basser and Pierpaoli (1996). The $b = 0$ scans were used to construct a T2-weighted image.

2.3. Region of interest

To better understand the relationship between aging and changes in white matter in the region of the perforant pathway, we manually segmented the PWM as a ROI using a previously described and validated protocol (Rogalski et al., 2009). Fig. 1 shows a sample tracing of the PWM ROI on a single coronal MR image. The Analyze software package (Mayo Clinic Foundation, Rochester, MN, USA) was used for segmenting the ROI boundaries and for estimating the volumes of each ROI. ROIs were traced bilaterally for each subject on the high resolution T1 weighted 3D-SPGR scan.

The PWM ROI boundaries were delineated on coronal slices. Tracing of the PWM began with the slice in which the gyrus ambiens, amygdala and white matter of the parahippocampal gyrus were first seen. The most caudal slice traced was one slice rostral to the first appearance of the lateral geniculate nucleus. The lateral border of the PWM was defined as the bend that signifies the junction between the PWM and the temporal stem. The medial border was defined as the point at which the white matter meets the gray matter of the entorhinal cortex. PWM tracings were carried out by ER (who was trained to be within 95% of LdeTM). All tracings were checked, slice by slice, by LdeTM.

To correct for individual differences in brain size, the PWM ROI volumes were divided by total intracranial volume derived from sagittally formatted 5 mm slices (i.e., normalized). To compute intracranial volume, the inner table of the cranium was traced (by ER and TS) in consecutive sagittal sections spanning the entire brain. At the level of the foramen magnum, a straight line was drawn from the inner surface of the clivus to the occipital bone. Normalized volume for brain regions of interest was determined using the formula:

$$(\text{absolute volume in mm}^3 / \text{intracranial volume in mm}^3) \times 1000.$$

For DTI and tractography analyses, the PWM ROIs were converted to SPM5 format for co-registration with the SPGR structural scan and the DTI scan for each participant. This conversion requires the application of the transformation matrix from the SPGR to the ROI for location alignment and re-slicing of the ROI to backfill the volume. The co-registration of the ROI to the SPGR and DTI scans utilized a rigid-body method as implemented in SPM5 which translates and rotates the SPGR volume to best match the DTI image. The co-registration parameters were applied to the PWM ROIs to bring them into anatomical alignment with the DTI data. No DTI metric was shifted during the co-registration to minimize the addition of noise associated with the registration process to the DTI images. Each co-registered SPGR and ROI were manually inspected for registration error and corrected when required. The DTI values within the PWM ROIs were extracted for each subject using software developed in our laboratory. While a number of DTI scalars are available for analysis, we used the most commonly cited measures of MD and FA.

Following DTI ROI analyses, the PWM ROIs were used as seed points to generate DTI derived tractographic models of the white matter pathways to measure the diffusion properties of the fibers passing through the PWM region. To generate the tractographic models, we used an open source suite of software developed at Stanford University (<http://siri.stanford.edu/software>) with modifications developed in our laboratory. These models were developed using a deterministic streamline tracking technique (Basser, Pajevic, Pierpaoli, Duda, & Aldroubi, 2000; Conturo et al., 1999; Lori et al., 2002; Mori, Crain, Chacko, & van Zijl, 1999) with Runge–Kutta 4th order integration (Thottakara, Lazar, Johnson, & Alexander, 2006). This algorithm seeks to propagate tracks based on the principal direction between voxels and on the primary eigenvector. The program assesses the degree of coherence between associated voxels in both a forward and a backward marching method. The model of the underlying white matter tracts is based on the highest directional association across voxels with a fiber termination at an FA value of less than 0.20, or an angular displacement of greater than 20°. From these models, we quantified the DTI metrics of MD and FA. These values were calculated individually for each participant based on the modeled tracts propagated from the individually determined PWM ROI.

2.4. Neuropsychological testing

Episodic memory function was tested using the verbal version of the Buschke controlled learning task (Buschke & Grober, 1986). This task distinguishes between “apparent” and “genuine” memory deficits in elderly individuals, since it controls for attention or the use of inefficient strategies in acquiring information. Using this task, previous work from our laboratory has demonstrated a material-specific relation between memory performance and hippocampal volume in patients with mild AD (deToledo-Morrell et al., 2000). Participants were asked to learn a list of 16 items presented four at a time as previously described (deToledo-Morrell et al., 2000). Items were shown as line drawings with one picture in each quadrant of a card. When a category cue was given verbally, the subject had to search, point to and *name* the object from that category. After this was done for four items, immediate

cued recall of the four items was tested by presenting each category cue to the subject. If the subject failed to recall an item in response to its cue, the item was shown again, and the entire process was repeated until immediate cued recall was correct for the four items. Then, the next set of four items was presented until all 16 items were correctly retrieved during immediate cued recall. The search and naming procedure ensured that all participants used the same strategy in processing information and that the items were correctly encoded.

After the subjects learned the items, three trials of free recall were administered, with each trial being preceded by 20 s of interference. On each trial, subjects were allowed a maximum of 2 min to name as many of the learned items as possible. Next, a category cue was provided for each item missed on that trial. If the subject still failed to recall the item with the cue, he/she was reminded of the missed item and asked to repeat it. An additional trial of free recall was administered after approximately 60 min to test for delayed recall.

2.5. Statistical analyses

Demographic differences between the two groups of participants were examined by independent two-tailed *t*-tests or *chi-square* analyses, as appropriate, in SPSS (SPSS, Chicago, IL). Separate independent two-tailed *t*-tests were used to examine group differences in MMSE, episodic memory performance, PWM volume, DTI metrics (FA, MD) of the PWM ROI and of the modeled white matter fiber tracts. Homogeneity of variance between the two groups was examined using Levene's test for equality of variances. This technique tests for differences in the variance structures between groups, and if significant differences are found, provides a protected significance value. Because of the number of repeated comparisons, we adopted a conservative statistical threshold of $p = 0.01$ for these analyses. The relative contribution of memory performance and imaging results to differentiating YNG and OLD groups was examined with logistic regression models. This technique identifies the relative strength of each predictor variable in classifying group membership. Likelihood ratios were used to assess the significance of each predictor for separating YNG and OLD groups. The likelihood ratio compares the $-2 \log$ likelihood from the base model, including only the intercept, to the $-2 \log$ likelihood of the expanded model with predictor variables. The likelihood ratio assumes a chi-square distribution.

3. Results

Yearly clinical examinations indicated that two of the older participants in the study had declined in cognitive status over a two-year follow-up period and had received a diagnosis of MCI. Therefore, the analyses presented below excluded these two individuals.

Demographic data, MMSE scores and episodic memory test scores are presented in Table 1. Examination of outcome variable homogeneity of variance between the young and old groups revealed a significant difference in variance structure only for FA values in the PWM region of interest [$F(1,39) = 16.38, p < 0.001$]. The two groups of participants did not differ in education [$t(38) = 0.05, p = 0.96$] or MMSE score [$t(38) = 0.68, p = 0.50$], but there were group differences in performance for verbal free recall after the third trial [$t(38) = 4.18, p < 0.001$] of the Buschke task and verbal delayed recall [$t(38) = 4.74, p < 0.001$].

3.1. Structural changes

PWM Volume—Total (right+left) PWM volume was extracted for each subject, adjusted for total intracranial volume (normalized), and compared by group. Results showed that total PWM volume was significantly reduced in the OLD compared to the YNG group [$t(38) = 4.50, p < 0.001$].

PWM DTI Metrics—The integrity of the white matter fibers in the region of the perforant pathway was assessed by comparing PWM ROI values for MD and FA between the two age groups. There was no significant difference in MD [$t(38) = 1.63, p = 0.11$]; however, FA was significantly higher in the YNG compared to the OLD group [$t(38) = 3.39, p = 0.03$ (protected significance value); see Fig. 2]. These results suggest that there are age-related changes in the parallel organization of remaining fibers, but not the general tissue structure in the OLD compared to the YNG group.

PWM Tractography Metrics—Thus far, we have reported changes in the PWM ROI, but not the tractography results assessing the fibers passing through this region. We used the PWM ROI as seed points to generate maps of fiber tracts (Fig. 3). Although there were PWM volume changes between the two age groups, the tractography method used reliably generated tracts for all subjects. To examine group differences as determined by the tractography results, we assessed MD and FA of the fibers passing through the PWM ROI. Results indicated no significant differences between the two groups for either of the DTI metrics [MD: $t(38) = 0.40, p = 0.97$; FA: $t(38) = 1.244, p = 0.22$]. The finding of no group differences in the DTI metrics of fiber pathways passing through the PWM is in contrast to age-related DTI changes found in the PWM ROI analyses described above, suggesting that such changes are best detected within the PWM region, rather than extending to the *fibers emanating from the region*.

3.2. Group classification

To examine models of group classification, we developed separate logistic regression analyses using measures that were significantly different between the YNG and OLD groups in univariate analyses, i.e., memory performance measures (the *third trial of free verbal recall, delayed verbal recall*), PWM ROI volume and DTI indices of PWM integrity (ROI FA) as predictors. Likelihood ratios (LR) were used to assess the relative contribution of each variable to the models. All logistic regression models were significant with delayed verbal recall as the most significant (LR = 17.86, $p < 0.0005$), followed by PWM ROI volume (LR = 16.19, $p < 0.0005$), third trial of free verbal recall (LR = 14.49, $p < 0.0005$) and PWM ROI FA (LR = 11.43, $p = 0.001$). When all four predictor variables were included in a single analysis, performance on the third trial of free verbal recall was dropped from the model. The subsequent model that included delayed verbal recall, PWM ROI volume and DTI ROI FA was highly significant (LR = 55.35, $p < 0.0005$), with an overall sensitivity and specificity of group classification of 95.2%.

4. Discussion

The present study characterized age-related changes in white matter integrity in vivo in the PWM region that includes the perforant pathway using volumetry, DTI and tractography. Our results demonstrate that, in addition to volume changes in the PWM region that includes the perforant pathway as reported by us previously (Stoub et al., 2011), there are micro-structural alterations in remaining fibers that may be occurring as a result of the *normal* aging process. More specifically, results reported here show significant differences in PWM volume and FA, but not in MD. With respect to tractography findings in DTI metrics of the fibers that pass through the PWM region, there were no significant differences between the age groups. In addition, PWM volume, along with delayed verbal recall and PWM FA were significant predictors of group membership (YNG or OLD), suggesting that maintaining proper flow of information from the entorhinal cortex to the hippocampus is important for episodic memory function.

The age-related change in FA observed in the present study suggests that there may be a loss in the parallel organization (or directional diffusion) of remaining PWM fibers as a result of

the aging process. These age-related alterations could be due to pruning of afferent and efferent fibers, axonal loss, as well as to partial demyelination. DTI metric data allow the detection of micro-structural abnormalities; however, they cannot provide an exact mechanism that may underlie these changes.

One possible mechanism postulated by Bartzokis, Lu and Mintz (2004), is that late myelinating regions of the brain, such as the PWM, are more susceptible to myelin breakdown later in life than early myelinating regions. This process of retrogenesis, whereby degenerative mechanisms reverse the order of acquisition in normal development, has been addressed in previous papers on aging and Alzheimer's disease (Brickman et al., 2011; Reisberg et al., 1999, 2002). Recent data from Stricker et al. (2009) support this hypothesis by showing significantly lower FA in patients with Alzheimer's disease in late myelinating, but not early myelinating pathways.

Previous studies of healthy aging have reported age-related structural changes in white matter (Raz et al., 1997; Salat et al., 2009, 2005; Sullivan & Pfefferbaum, 2006; Sullivan, Rohlfing, & Pfefferbaum, 2010; Tisserand, Visser, van Boxtel, & Jolles, 2000; Voineskos et al., 2010), but, to our knowledge, only one focused specifically on the perforant pathway region of the PWM using DTI (Yassa et al., 2010). In that report, DTI scans were acquired with an ultrahigh resolution protocol, but with gaps between slices that limits the measurement of volume. As acknowledged by Yassa (2011), although the in-plane resolution of this protocol was high, the through-plane resolution was poor, leading to possible partial volume contamination. Employing a metric of diffusion not previously used, these investigators found signal degradation in the perforant pathway in older adults compared with young participants. Our results complement and extend the findings of this study by including PWM volume as an outcome measure, as well as by reporting the commonly reported DTI parameters of FA and MD using a gapless acquisition protocol.

Distinguishing genuine aging effects in cross-sectional investigations is complex since some of the healthy cohort entering a study may be in the pre-clinical stages of AD. Fortunately, our healthy older participants are part of an ongoing longitudinal study that involves yearly clinical follow-up. Because of such follow-up, we were able to detect decline to MCI in two of our old participants and removed them from the analyses reported here. The analyses are based on the baseline scans of old participants who remained stable as healthy old controls over a four year follow-up period.

In summary, results reported here demonstrate that in addition to the age-related volume reduction in the PWM that includes the perforant pathway, there are micro-structural changes in remaining fibers, although to a lesser extent than in prodromal and mild AD. These data support the hypothesis that age-related decline in memory performance may partly be a consequence of a partial disconnection in the flow of information from the entorhinal cortex to the hippocampus via the perforant pathway. It is remarkable that the age-related change in white matter in the region of the perforant pathway in humans resembles that found in aging rodents and suggests that this alteration may be fundamental to brain aging across mammalian species.

Acknowledgments

This work was supported by Grants P01 AG09466 and P30 AG10161 from the National Institute on Aging, National Institutes of Health, the Illinois Department of Public Health and the McKnight Brain Research Foundation. The authors wish to thank Roland Bammer, Ph.D. and Michael E. Moseley, Ph.D. from Stanford University for supplying the pulse sequence used in the diffusion tensor imaging scans.

References

- Abe O, Yamasue H, Aoki S, Suga M, Yamada H, Kasai K, et al. Aging in the CNS: Comparison of gray/white matter volume and diffusion tensor data. *Neurobiology of Aging*. 2008; 29:102–116. [PubMed: 17023094]
- Amaral DG, Insausti R, Cowan WM. The entorhinal cortex of the monkey: I. Cytoarchitectonic organization. *Journal of Comparative Neurology*. 1987; 264:326–355. [PubMed: 2445795]
- Barnes CA. Memory deficits associated with senescence: A neurophysiological and behavioral study in the rat. *Journal of Comparative and Physiological Psychology*. 1979; 93:74–104. [PubMed: 221551]
- Barnes CA, McNaughton BL. Physiological compensation for loss of afferent synapses in rat hippocampal granule cells during senescence. *Journal of Physiology*. 1980; 309:473–485. [PubMed: 7252877]
- Bartzokis G, Lu PH, Mintz J. Quantifying age-related myelin breakdown with MRI: Novel therapeutic targets for preventing cognitive decline and Alzheimer's disease. *Journal of Alzheimer's Disease: JAD*. 2004; 6:S53–59.
- Basser PJ, Mattiello J, LeBihan D. Estimation of the effective self-diffusion tensor from the NMR spin echo. *Journal of Magnetic Resonance Series B*. 1994; 103:247–254. [PubMed: 8019776]
- Basser PJ, Pajevic S, Pierpaoli C, Duda J, Aldroubi A. In vivo fiber tractography using DT-MRI data. *Magnetic Resonance in Medicine*. 2000; 44:625–632. [PubMed: 11025519]
- Basser PJ, Pierpaoli C. Microstructural and physiological features of tissues elucidated by quantitative-diffusion-tensor MRI. *Journal of Magnetic Resonance Series B*. 1996; 111:209–219. [PubMed: 8661285]
- Brickman AM, Meier IB, Korgaonkar MS, Provenzano FA, Grieve SM, Siedlecki KL, et al. Testing the white matter retrogenesis hypothesis of cognitive aging. *Neurobiology of Aging*. 2011 Epub ahead of print.
- Buschke H, Grober E. Genuine memory deficits in age-associated memory impairment. *Developmental Neuropsychology*. 1986; 2:287–307.
- Conturo TE, Lori NF, Cull TS, Akbudak E, Snyder AZ, Shimony JS, et al. Tracking neuronal fiber pathways in the living human brain. *Proceedings of the National Academy of Sciences of the United States of America*. 1999; 96:10422–10427. [PubMed: 10468624]
- deToledo-Morrell L, Dickerson B, Sullivan MP, Spanovic C, Wilson R, Bennett DA. Hemispheric differences in hippocampal volume predict verbal and spatial memory performance in patients with Alzheimer's disease. *Hippocampus*. 2000; 10:136–142. [PubMed: 10791835]
- deToledo-Morrell L, Stoub TR, Bulgakova M, Wilson RS, Bennett DA, Leurgans S, et al. MRI-derived entorhinal volume is a good predictor of conversion from MCI to AD. *Neurobiology of Aging*. 2004; 25:1197–1203. [PubMed: 15312965]
- Folstein MF, Folstein SE, McHugh PR. "Mini-mental state". A practical method for grading the cognitive state of patients for the clinician. *Journal of Psychiatric Research*. 1975; 12:189–198. [PubMed: 1202204]
- Geinisman Y, deToledo-Morrell L, Morrell F. Loss of perforated synapses in the dentate gyrus: Morphological substrate of memory deficit in aged rats. *Proceedings of the National Academy of Sciences of the United States of America*. 1986; 83:3027–3031. [PubMed: 3458260]
- Geinisman Y, deToledo-Morrell L, Morrell F, Persina IS, Rossi M. Age-related loss of axospinous synapses formed by two afferent systems in the rat dentate gyrus as revealed by the unbiased stereological disector technique. *Hippocampus*. 1992; 2:437–444. [PubMed: 1308200]
- Huang J, Auchus AP. Diffusion tensor imaging of normal appearing white matter and its correlation with cognitive functioning in mild cognitive impairment and Alzheimer's disease. *Annals of the New York Academy of Sciences*. 2007; 1097:259–264. [PubMed: 17413027]
- Huang J, Friedland RP, Auchus AP. Diffusion tensor imaging of normal-appearing white matter in mild cognitive impairment and early Alzheimer disease: Preliminary evidence of axonal degeneration in the temporal lobe. *AJNR American Journal of Neuroradiology*. 2007; 28:1943–1948. [PubMed: 17905894]

- Hyman BT, Van Hoesen GW, Damasio AR, Barnes CL. Alzheimer's disease: Cell-specific pathology isolates the hippocampal formation. *Science*. 1984; 225:1168–1170. [PubMed: 6474172]
- Kalus P, Slotboom J, Gallinat J, Mahlberg R, Cattapan-Ludewig K, Wiest R, et al. Examining the gateway to the limbic system with diffusion tensor imaging: The perforant pathway in dementia. *Neuroimage*. 2006; 30:713–720. [PubMed: 16337815]
- Kantarci K, Senjem ML, Avula R, Zhang B, Samikoglu AR, Weigand SD, et al. Diffusion tensor imaging and cognitive function in older adults with no dementia. *Neurology*. 2011; 77:26–34. [PubMed: 21593440]
- Lori NF, Akbudak E, Shimony JS, Cull TS, Snyder AZ, Guillory RK, et al. Diffusion tensor fiber tracking of human brain connectivity: Acquisition methods, reliability analysis and biological results. *NMR in Biomedicine*. 2002; 15:494–515. [PubMed: 12489098]
- Malykhin N, Vahidy S, Michielse S, Coupland N, Camicioli R, Seres P, et al. Structural organization of the prefrontal white matter pathways in the adult and aging brain measured by diffusion tensor imaging. *Brain Structure and Function*. 2011; 216:417–431. [PubMed: 21559982]
- Medina D, deToledo-Morrell L, Urresta F, Gabrieli JD, Moseley M, Fleischman D, et al. White matter changes in mild cognitive impairment and AD: A diffusion tensor imaging study. *Neurobiology of Aging*. 2006; 27:663–672. [PubMed: 16005548]
- Mori S, Crain BJ, Chacko VP, van Zijl PC. Three-dimensional tracking of axonal projections in the brain by magnetic resonance imaging. *Annals of Neurology*. 1999; 45:265–269. [PubMed: 9989633]
- Morris JC, Heyman A, Mohs RC, Hughes JP, van Belle G, Fillenbaum G, et al. The consortium to establish a registry for Alzheimer's disease (CERAD). Part I. Clinical and neuropsychological assessment of Alzheimer's disease. *Neurology*. 1989; 39:1159–1165. [PubMed: 2771064]
- Moseley M. Diffusion tensor imaging and aging—A review. *NMR in Biomedicine*. 2002; 15:553–560. [PubMed: 12489101]
- Pfefferbaum A, Sullivan EV, Hedehus M, Lim KO, Adalsteinsson E, Moseley M. Age-related decline in brain white matter anisotropy measured with spatially corrected echo-planar diffusion tensor imaging. *Magnetic Resonance in Medicine*. 2000; 44:259–268. [PubMed: 10918325]
- Rasmussen T, Schliemann T, Sorensen JC, Zimmer J, West MJ. Memory impaired aged rats: No loss of principal hippocampal and subicular neurons. *Neurobiology of Aging*. 1996; 17:143–147. [PubMed: 8786797]
- Raz N, Gunning FM, Head D, Dupuis JH, McQuain J, Briggs SD, et al. Selective aging of the human cerebral cortex observed in vivo: Differential vulnerability of the prefrontal gray matter. *Cerebral Cortex*. 1997; 7:268–282. [PubMed: 9143446]
- Reisberg B, Franssen EH, Hasan SM, Monteiro I, Boksay I, Souren LE, et al. Retrogenesis: Clinical, physiologic, and pathologic mechanisms in brain aging, Alzheimer's and other dementing processes. *European Archives of Psychiatry and Clinical Neuroscience*. 1999; 249(Suppl. 3):28–36. [PubMed: 10654097]
- Reisberg B, Franssen EH, Souren LE, Auer SR, Akram I, Kenowsky S. Evidence and mechanisms of retrogenesis in Alzheimer's and other dementias: Management and treatment import. *American Journal of Alzheimer's Disease and Other Dementias*. 2002; 17:202–212.
- Rogalski EJ, Murphy CM, deToledo-Morrell L, Shah RC, Moseley ME, Bammer R, et al. Changes in parahippocampal white matter integrity in amnesic mild cognitive impairment: A diffusion tensor imaging study. *Behavioral Neurology*. 2009; 21:51–61. [PubMed: 19847045]
- Rohde GK, Barnett AS, Basser PJ, Marengo S, Pierpaoli C. Comprehensive approach for correction of motion and distortion in diffusion-weighted MRI. *Magnetic Resonance in Medicine*. 2004; 51:103–114. [PubMed: 14705050]
- Salat DH, Tuch DS, Greve DN, van der Kouwe AJ, Hevelone ND, Zaleta AK, et al. Age-related alterations in white matter microstructure measured by diffusion tensor imaging. *Neurobiology of Aging*. 2005; 26:1215–1227. [PubMed: 15917106]
- Salat DH, Greve DN, Pacheco JL, Quinn BT, Helmer KG, Buckner RL, et al. Regional white matter volume differences in nondemented aging and Alzheimer's disease. *Neuroimage*. 2009; 44:1247–1258. [PubMed: 19027860]

- Salat DH, Tuch DS, van der Kouwe AJ, Greve DN, Pappu V, Lee SY, et al. White matter pathology isolates the hippocampal formation in Alzheimer's disease. *Neurobiology of Aging*. 2010; 31:244–256. [PubMed: 18455835]
- Sasoon E, Doniger GM, Pasternak O, Tarrasch R, Assaf Y. Structural correlates of cognitive domains in normal aging with diffusion tensor imaging. *Brain Structure and Function*. 2011 Epub ahead of print.
- Smith TD, Adams MM, Gallagher M, Morrison JH, Rapp PR. Circuit-specific alterations in hippocampal synaptophysin immunoreactivity predict spatial learning impairment in aged rats. *Journal of Neuroscience*. 2000; 20:6587–6593. [PubMed: 10964964]
- Squire LR, Zola-Morgan S. The medial temporal lobe memory system. *Science*. 1991; 253:1380–1386. [PubMed: 1896849]
- Stoub TR, Bulgakova M, Leurgans S, Bennett DA, Fleischman D, Turner DA, et al. MRI predictors of risk of incident Alzheimer disease: A longitudinal study. *Neurology*. 2005; 64:1520–1524. [PubMed: 15883311]
- Stoub TR, deToledo-Morrell L, Stebbins GT, Leurgans S, Bennett DA, Shah RC. Hippocampal disconnection contributes to memory dysfunction in individuals at risk for Alzheimer's disease. *Proceedings of the National Academy of Sciences of the United States of America*. 2006; 103:10041–10045. [PubMed: 16785436]
- Stoub TR, Rogalski EJ, Leurgans S, Bennett DA, deToledo-Morrell L. Rate of entorhinal and hippocampal atrophy in incipient and mild AD: Relation to memory function. *Neurobiology of Aging*. 2010; 31:1089–1098. [PubMed: 18809228]
- Stoub TR, Barnes CA, Shah RC, Stebbins GT, Ferrari C, deToledo-Morrell L. Age-related changes in the mesial temporal lobe: The parahippocampal white matter region. *Neurobiology of Aging*. 2011 E-pub ahead of print.
- Stricker NH, Schweinsburg BC, Delano-Wood L, Wierenga CE, Bangen KJ, Haaland KY, et al. Decreased white matter integrity in late-myelinating fiber pathways in Alzheimer's disease supports retrogenesis. *Neuroimage*. 2009; 45:10–16. [PubMed: 19100839]
- Sullivan EV, Pfefferbaum A. Diffusion tensor imaging and aging. *Neuroscience and Biobehavioral Reviews*. 2006; 30:749–761. [PubMed: 16887187]
- Sullivan EV, Rohlfing T, Pfefferbaum A. Quantitative fiber tracking of lateral and interhemispheric white matter systems in normal aging: Relations to timed performance. *Neurobiology of Aging*. 2010; 31:464–481. [PubMed: 18495300]
- Thottakara P, Lazar M, Johnson SC, Alexander AL. Application of Brodmann's area templates for ROI selection in white matter tractography studies. *Neuroimage*. 2006; 29:868–878. [PubMed: 16243544]
- Tisserand DJ, Visser PJ, van Boxtel MP, Jolles J. The relation between global and limbic brain volumes on MRI and cognitive performance in healthy individuals across the age range. *Neurobiology of Aging*. 2000; 21:569–576. [PubMed: 10924774]
- Van Hoesen G, Pandya DN. Some connections of the entorhinal (area 28) and perirhinal (area 35) cortices of the rhesus monkey. I. Temporal lobe afferents. *Brain Research*. 1975a; 95:1–24. [PubMed: 1156859]
- Van Hoesen G, Pandya DN. Some connections of the entorhinal (area 28) and perirhinal (area 35) cortices of the rhesus monkey. III. Efferent connections. *Brain Research*. 1975b; 95:39–59. [PubMed: 1156868]
- Van Hoesen G, Pandya DN, Butters N. Some connections of the entorhinal (area 28) and perirhinal (area 35) cortices of the rhesus monkey. II. Frontal lobe afferents. *Brain Research*. 1975; 95:25–38. [PubMed: 1156867]
- Voineskos AN, Rajji TK, Lobaugh NJ, Miranda D, Shenton ME, Kennedy JL, et al. Age-related decline in white matter tract integrity and cognitive performance: A DTI tractography and structural equation modeling study. *Neurobiology of Aging*. 2010 E-pub ahead of print.
- Wang C, Stebbins GT, Medina DA, Shah RC, Bammer R, Moseley ME, et al. Atrophy and dysfunction of parahippocampal white matter in mild Alzheimer's disease. *Neurobiology of Aging*. 2010 E-pub ahead of print.

- Yassa MA, Muftuler LT, Stark CE. Ultrahigh-resolution microstructural diffusion tensor imaging reveals perforant path degradation in aged humans in vivo. *Proceedings of the National Academy of Sciences of the United States of America*. 2010; 107:12687–12691. [PubMed: 20616040]
- Yassa MA. Searching for biomarkers using high resolution diffusion tensor imaging. *Journal of Alzheimer's Disease*. 2011; 26(Suppl. 3):297–305.
- Young BJ, Otto T, Fox GD, Eichenbaum H. Memory representation within the parahippocampal region. *Journal of Neuroscience*. 1997; 17:5183–5195. [PubMed: 9185556]

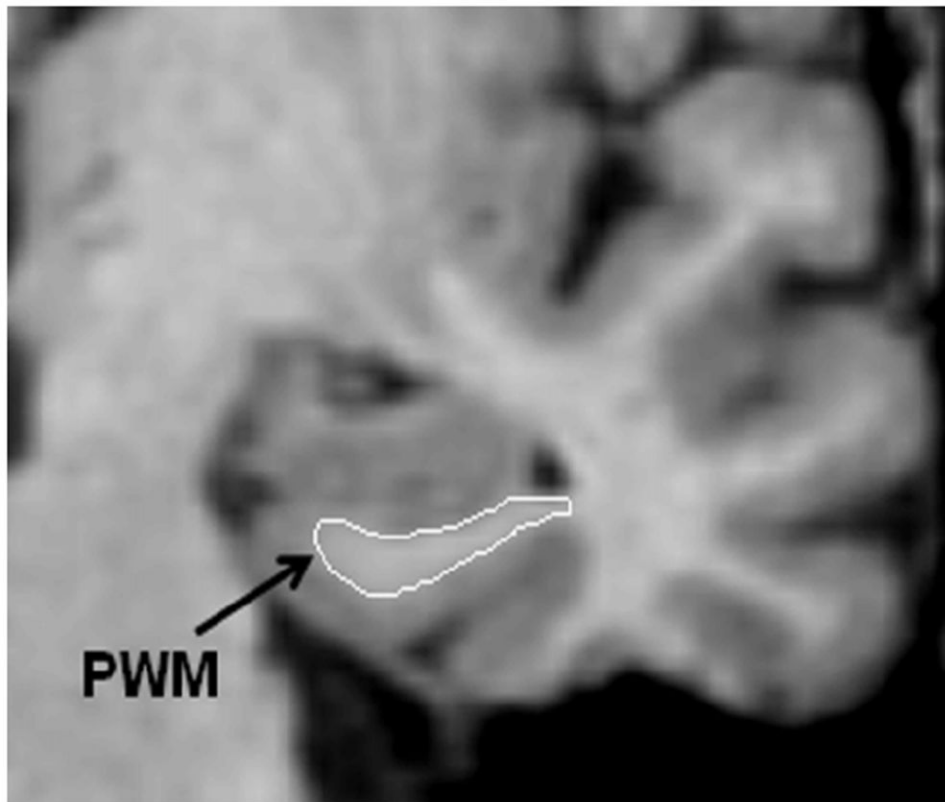


Fig. 1. A coronal SPGR image of the medial temporal lobe illustrating the segmentation of the parahippocampal white matter region of interest.

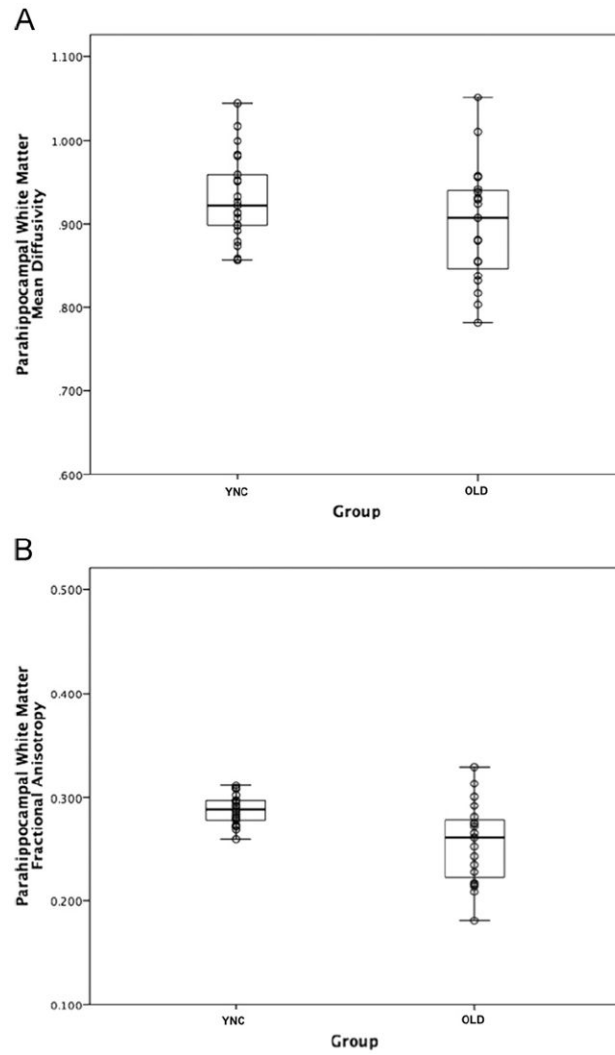


Fig. 2. Box plots of DTI metrics from the PWM region by groups. Panel A shows the distribution of MD within the PWM ROI for young (YNG) and the older (OLD) participants, while panel B shows the distribution of FA.

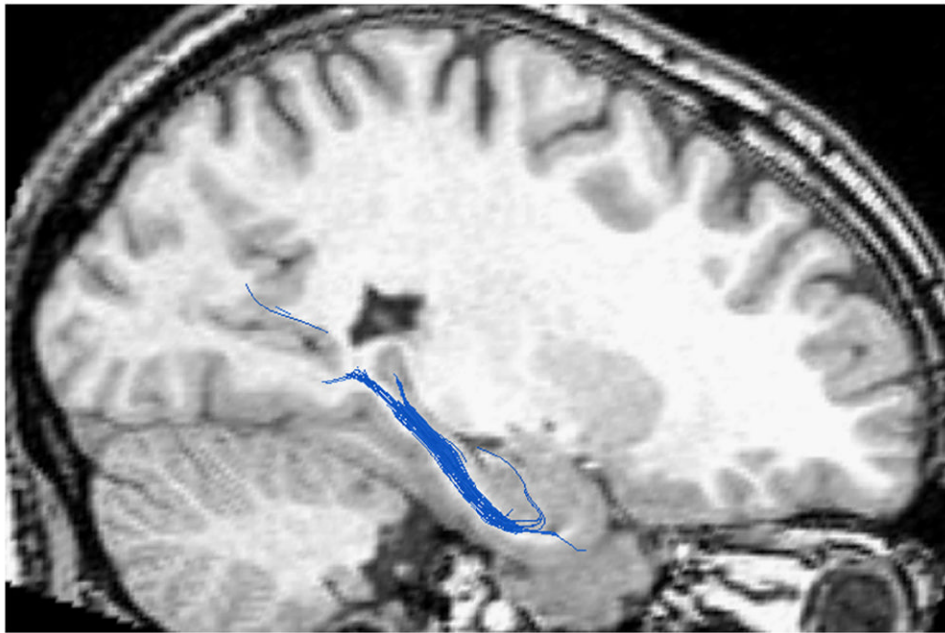


Fig. 3.
An example of the fiber tracts using the PWM ROI as a seed region.

Table 1

Demographic characteristics, MMSE and declarative memory scores of participants.

	YNG	OLD
Male: female	12:9	8:11
Age	24.8 (± 2.5)	71.1 (± 6.0)*
Education (years)	15.8 (± 1.9)	15.6 (± 2.3)
MMSE^a	29.1 (± 0.9)	29.4 (± 0.8)
Verbal recall following trial 3^b	84.7 (± 10.9)	71.1 (± 12.4)*
Verbal delayed recall^b	83.8 (± 11.0)	69.4 (± 11.6)*

* Significantly different from the young group ($p < 0.05$). Means and standard deviations are provided.

^a Mini Mental Status Exam (MMSE): the maximum score is 30 and 27 is considered normal.

^b Scores are expressed as percent correct.